BMC Biology

RESEARCH ARTICLE

Open Access

Early inhibition of BRD4 facilitates iPSC reprogramming via accelerating rDNA dynamic expression

Zhijing Zhang[1,2], Xinglin Hu[1], Yuchen Sun[1], Lei Lei[1*] and Zhonghua Liu[2*]

Abstract

Background iPSC reprogramming technology exhibits significant promise in the realms of clinical therapeutics, disease modeling, pharmaceutical drug discovery, and various other applications. However, the extensive utilization of this technology has encountered impediments in the form of inefficiency, prolonged procedures, and ambiguous biological processes. Consequently, in order to improve this technology, it is of great significance to delve into the underlying mechanisms involved in iPSC reprogramming. The BET protein BRD4 plays a crucial role in the late stage of reprogramming; however, its precise function in the early stage remains unclear.

Results Our study aims to investigate BRD4's role in the early stages of iPSC reprogramming. Our investigation reveals that early inhibition of BRD4 substantially enhances iPSC reprogramming, whereas its implementation during the middle-late stage impedes the process. During the reprogramming, ribosome DNA expression initially increases before decreasing and then gradually recovers. Early inhibition of BRD4 improved the decline and restoration of rDNA expression in the early and middle-late stages, respectively. Additionally, we uncovered the mechanism of BRD4's regulation of rDNA transcription throughout reprogramming. Specifically, BRD4 interacts with UBF and co-localizes to both the rDNA promoter and enhancer regions. Ultimately, BRD4 facilitates rDNA transcription by promoting the enrichment of histone H3 lysine 27 acetylation in the surrounding chromatin. Moreover, we also discovered that early inhibition of BRD4 facilitates cells' transition out of the somatic cell state and activate pluripotent genes.

Conclusions In conclusion, our results demonstrate that early inhibition of BRD4 promotes sequential dynamic expression of rDNA, which improves iPSC reprogramming efficiency.

Keywords BRD4, UBF, H3K27ac, IPSC reprogramming, RDNA expression, Epigenetics

Background

The Yamanaka factors have been demonstrated to induce the reprogramming of somatic cells into induced pluripotent stem cells (iPSCs) [1]. However, the limited application of iPSCs in various fields is due to their inefficiency, slow process, and uncertain safety [2]. In the process of iPSC reprogramming, a cascade of biological events occurs either sequentially or simultaneously. The failure of a considerable proportion of reprogramming cells can be attributed to the aberrant occurrence of these events. Previous studies have categorized these related key events into three distinct stages, each

*Correspondence:
Lei Lei
lei086@ems.hrbmu.edu.cn
Zhonghua Liu
liuzhonghua@neau.edu.cn
[1] Department of Histology and Embryology, Harbin Medical University, 157 Baojian Street, Nangang DistrictHeilongjiang Province 150086, Harbin, China
[2] Key Laboratory of Animal Cellular and Genetic Engineering of Heilongjiang Province, Northeast Agricultural University, 31 Mucai Street, Xiangfang DistrictHeilongjiang Province 150030, Harbin, China

of which plays a specific role in maintaining the reprogramming process. The early stage involves the downregulation of somatic cell-related genes and a decrease in chromatin accessibility [3–5]. During this stage, numerous specific accessible chromatin sites associated with somatic cell characteristics are rapidly closing, thereby triggering a pronounced decrease in the expression of these genes during the initial transcription wave [1, 3, 6]. Furthermore, a pivotal biological event, mesenchymal-to-epithelial transition (MET), occurs during this phase. Reprogramming cells undergoing the MET process transition from fibroblast-like to epithelial-like cells, accompanied by significant activation of gene expression, particularly in cell adhesion molecules such as Cdh1, also known as E-cadherin [7]. The intermediate stage is characterized by the activation of stem cell-related gene expression [8, 9]. Concurrently, with the activation of the second transcription wave, various pluripotent genes are significantly upregulated [6, 10]. The late stage entails the reorganization of chromatin structure with the assistance of various factors to establish the specific genome structure of iPSCs [11, 12].

BRD4, a critical factor in mammalian embryonic development, belongs to the bromodomain and extra-terminal (BET) protein family [13]. By recognizing and binding acetylated H3 and H4 of activated genes through its bromodomain, BRD4 recruits transcription factors such as positive transcription elongation factor b (P-TEFb) and others to regulate the expression of target genes [14–16]. Recent evidence has shown BRD4 enhances reprogramming efficiency in the late stage by recruiting and activating the P-TEFb complex, which stimulates productive transcriptional elongation of pluripotency genes [17]. Moreover, BRD4 upregulates gene transcription by binding to super-enhancers (SE) of ESC-specific genes in the OSKM plus with C/EBPα iPSC reprogramming system [18]. However, these studies have mainly focused on BRD4's function in the middle or late stage of reprogramming, while the early stage's role remains unknown.

In addition to participating in RNA polymerase II (Pol II)-mediated transcription, the association between BRD4 and ribosome DNA (rDNA) expression has garnered significant attention. Izumikawa et al. found that BRD4 can be recruited to rDNA by the LYAR-UBF complex and acetylated histone H4, facilitating rDNA transcription [19]. rDNA, a prototypical multicopy gene, is organized in arrays of tandem repeats distributed extensively along the short arms of chromosomes 12, 15, 16, 17, 18, and 19 in mice [20]. Transcription of rDNA is intricately linked with ribosome biogenesis, the central process of protein synthesis [21], thereby playing a pivotal role in modulating or altering cellular fate. Previous investigations have highlighted aberrations in rDNA expression across various developmental disorders, including amyotrophic lateral sclerosis (ALS), frontotemporal dementia (FTD), and Huntington's disease (HD) [22]. Additionally, pathological rDNA transcription has been implicated in tumorigenesis, encompassing conditions such as cervical intraepithelial neoplasia (CIN) and human hepatocellular carcinoma (HCC) [23]. Thus, it is evident that rDNA transcription significantly influences cellular fate. In the context of iPSC reprogramming, our prior research demonstrated that reactivation of rDNA via serum starvation markedly enhances iPSC reprogramming efficiency [24]. Furthermore, we previously demonstrated that transient downregulation of rDNA transcription in donor cells improves the preimplantation development of somatic cell nuclear transfer (SCNT) embryos [25]. Recently, Shi et al. also reported a significant disparity in rRNA levels between MEF and iPSC, along with dynamic expression alterations during reprogramming, using PANDORA-seq [26]. Altogether, they suggest a strong association between rDNA transcription and somatic reprogramming, including iPSC reprogramming and SCNT. Consequently, we hypothesize that BRD4 may influence iPSC reprogramming efficiency by regulating rDNA transcription.

In this study, we show that targeted degradation of BRD4 in the early phase markedly enhances mouse iPSC reprogramming by accelerating the dynamic alteration of rDNA expression. Furthermore, we uncover the mechanism by which BRD4 regulates rDNA expression during reprogramming. BRD4 interacts with UBF and co-localizes to the promoter and enhancer regions of rDNA, thereby facilitating the adjacent H3 lysine 27 acetylation (H3K27ac) modification to modulate transcriptional activity of rDNA. Additionally, early inhibition of BRD4 robustly reduces somatic gene expression in the early stage and activates pluripotent genes in the middle-late stage of reprogramming.

Results

Enhancing iPSC reprogramming efficiency by early inhibition of BRD4

Upon reviewing the previous RNA-seq data (GSE70022) and conducting RT-qPCR analysis, we confirmed that iPSCs had higher Brd4 expression than MEFs, consistent with previous report (Additional file 1: Fig. S1A, S1B) [17, 27, 28]. We then examined the mRNA and protein expression track of BRD4 and found that both gradually increased in the process of iPSC reprogramming (Additional file 1: Fig. S1C). A study by Liu et al. suggested that BRD4 plays a crucial role in the late stage of iPSC reprogramming. Therefore, we speculated that the gradual increased BRD4 expression may be indicative of preparing for the role to be played in the late stage. However, another report indicated

that inhibition of BET proteins during early reprogramming could improve iPSC efficiency [29]. Regrettably, this study did not delve into the specific functions of individual members. This hence prompted us to explore whether early suppression of BRD4 could also enhance iPSC reprogramming efficiency, even if Brd4 continues to increase during the process. Since cell viability is critical for iPSC reprogramming, we aimed to identify an experimental condition that could significantly degrade BRD4 while maintaining cell viability. Figure 1 A shows that 1.5 μM AT6, a specific BRD4 degrader [30], significantly degraded BRD4 in iPSC cells within 48 h (Fig. 1A). Additionally, Cell Counting Kit-8 (CCK8) experiment demonstrated that this condition minimally impaired cell viability (Fig. 1B). We treated 4F2A MEFs with either DMSO or AT6 under this condition on D0 and D2. Alkaline phosphatase (AP) staining revealed a noteworthy enhancement in reprogramming efficiency within the AT6-treated groups on reprogramming D8, contrasting with the limited effect observed in the DMSO-treated group (Fig. 1C). To ensure the reproducibility of our findings across different reprogramming systems, we repeated the experiment using the OSKM-virus reprogramming system and observed similar results (Additional file 1: Fig. S1D). We also confirmed that the AT6-treated iPSCs contained normal pluripotency and differentiation potential (Additional file 1: Fig. S1E, S1F). However, as Liu et al. have reported, knockdown of BRD4 during the late stage of reprogramming can significantly interfere with iPSC occurrence [17]. Therefore, we speculated that inhibiting BRD4 at different time points might result in different reprogramming efficiencies. To test this hypothesis, we inhibited BRD4 in D4 and D6, respectively, and performed AP staining in D8. As expected, the reprogramming efficiency of AT6 group was notably impaired (Fig. 1D). We also examined the expression of pluripotent genes under different conditions. When BRD4 was inhibited in D0, all the pluripotent genes were activated in D6 (Fig. 1E). Conversely, when treated with AT6 in D4, pluripotent gene expression was markedly downregulated in D6 (Fig. 1F). And in D8, despite Nanog expression is nearly restored, other pluripotent genes are still inactivated after treated with AT6 in D4 (Fig. 1G). In conclusion, our findings suggest that degrading BRD4 in D0 can activate pluripotent genes therefore improving reprogramming efficiency. In contrast, inhibiting BRD4 in D4 would significantly impair both the reprogramming efficiency and pluripotent gene expression.

The correlation between rDNA expression and BRD4 during reprogramming

Based on the aforementioned results, it is apparent that inhibiting BRD4 at different time points diversely affects reprogramming efficiency, possibly due to the varying roles that BRD4 plays at different stages of reprogramming. However, given the heterogeneity of different reprogramming systems, there is no universal indicator of iPSC reprogramming stage for now. To address this issue, we reanalyzed our RNA-seq data from iPSC reprogramming (GSE227745) and utilized hierarchical clustering to determine the stage of reprogramming [31]. Results showed that D6 was more closely related to the D8 state, while D4 cells were in a transitional state between somatic state (D2) and pluripotent state (D6 and D8) (Fig. 2A). Additionally, principal component analysis (PCA) was employed to identify the trajectory of reprogramming (Fig. 2B). Results from the PCA revealed that our reprogramming process followed an indirect route towards pluripotency, which is consistent with previous studies [6, 32]. Furthermore, D4 was also identified as a pivotal intermediate stage during the conversion of somatic cells to pluripotent cells [6, 32]. Moreover, cells in reprogramming D4 displayed typical MET morphology (Fig. 2C), which is considered a landmark event at the boundary between the early and middle stages of iPSC reprogramming [7, 33]. Given that somatic cell identity loss in the early stage is one of the first critical steps in iPSC reprogramming, we considered D0–D4 as the early stage and the rest as the middle-late stage. When BRD4 was inhibited in the early stage, we speculated that a large number of biological processes involved in the reprogramming might be altered, thereby affecting reprogramming efficiency. Our laboratory has previously demonstrated that early downregulation of rDNA expression is closely associated with somatic reprogramming efficiency [24, 25, 34]. Interestingly, in 293 T cells, BRD4 was found to bind to rDNA via LYAR-UBF complex and regulate rDNA transcription [19]. Therefore, it was possible that loss of BRD4 might alter rDNA transcription. To validate this hypothesis, we assessed rDNA expression, including 47 s and 18 s transcripts, and evaluated the rate of rRNA processing, as indicated by the 18 s/47 s ratio, at various time points, using RT-qPCR. We observed an initial transient and rapid increase in rDNA expression, likely stimulated by Yamanaka factors, followed by a gradual decrease. However, the transcription finally restored to a high level to accommodate the increased protein translation demand for iPSC (Fig. 2D). This finding indicated that rDNA expression decrease might be a critical event for iPSC reprogramming. Therefore, we performed AT6 to explore the impact of early BRD4 loss on rDNA transcription. Western blotting results showed that upon AT6 treatment at D0, BRD4 was degraded until D4 and restored to normal levels by D6 (Fig. 2E–F). Furthermore, 47 s, 18 s, and the rate of rRNA processing were quantified by RT-qPCR. After D0-AT6 treatment, in D2, the expression levels of 47S and 18S rRNAs

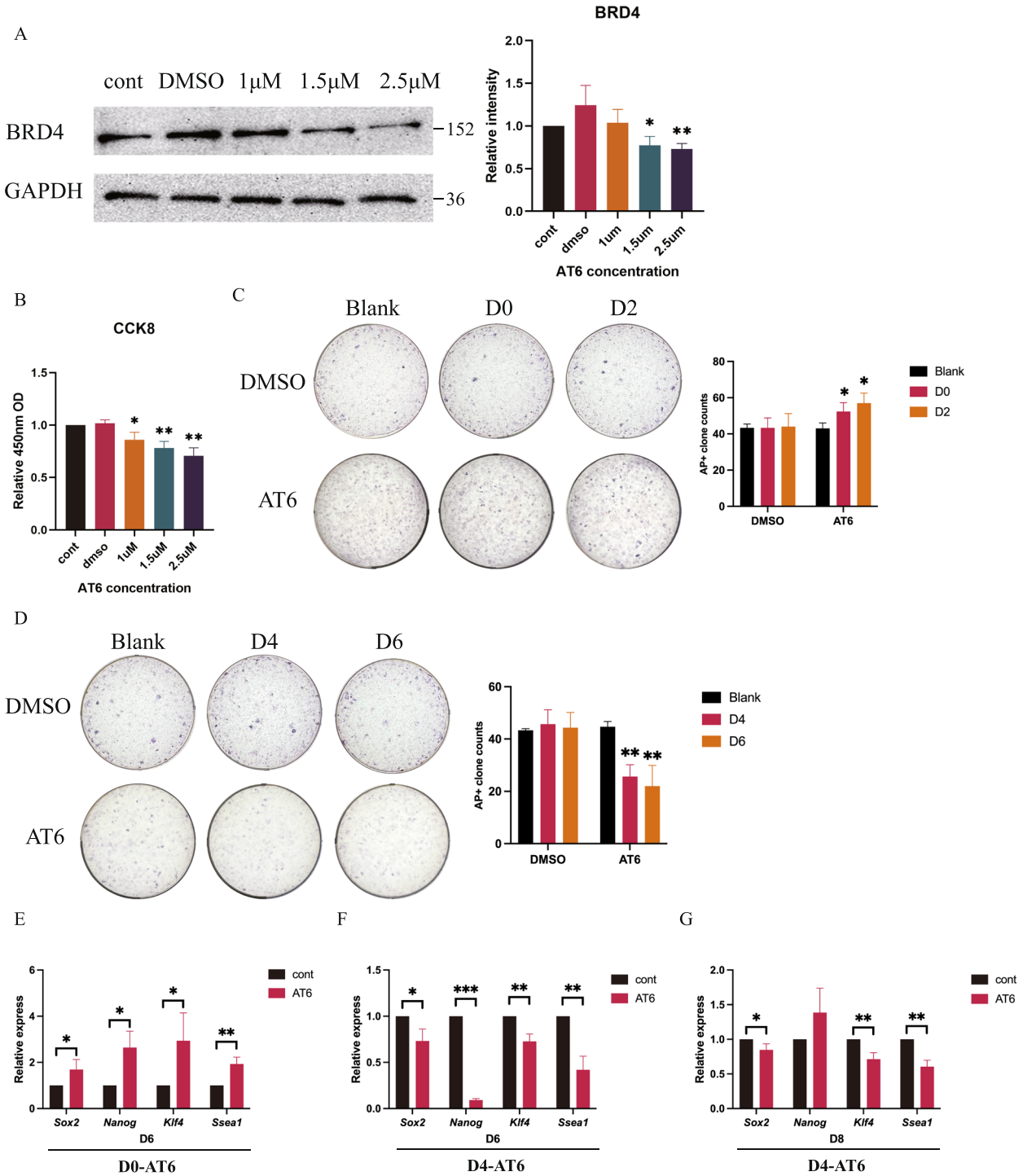

Fig. 1 Reprogramming efficiency varies with BRD4 degradation on different days. **A** BRD4 protein expression upon BRD4 inhibition at different concentrations. The bar plot shows statistical results of gray value. **B** CCK8 analysis of cell viability upon BRD4 inhibition at different concentrations. **C, D** AP staining and reprogramming efficiency analysis upon BRD4 inhibition at indicated times. The bar plots present the AP+ clone counts. **E** mRNA expression levels of pluripotent genes in control and D0-AT6 group at D6. **F, G** mRNA expression levels of pluripotent genes in control and D4-AT6 group at D6 and D8, respectively. All bars represent mean ± SD. ($n = 3$ independent experiments; *P<0.05, **P <0.01, ***P< 0.001, t test)

are downregulated, and the rate of rRNA processing begins to decrease, although it is not statistically significant at this point (Additional file 1: Fig. S2). By D4, both rDNA expression and rRNA processing rate are strikingly downregulated (Fig. 2G). The results suggest that early inhibition of BRD4 could strikingly reduce rDNA

transcription and rRNA processing rate in the early stage. However, by D6, rDNA transcription in the AT6-treated group is efficiently restored to an even higher level than that in the control group (Fig. 2H), suggesting that early inhibition of BRD4 could effectively expedite the dynamic expression of rDNA. As the ribosome is constituted by both rRNA and ribosome protein, we also investigated whether BRD4 loss could affect ribosome protein levels. However, western blotting results showed no significant alteration for S6 and pS6 expression upon BRD4 deficiency (Fig. 2E, 2I). These findings suggest that early inhibition of BRD4 specifically impairs rDNA transcription without affecting ribosome protein levels. We further investigate whether it could also expedite the dynamic expression of rDNA upon inhibition in the middle-late stage. After degrading BRD4 in D4, we analyzed rDNA transcription and 18 s/47 s rate by RT-qPCR. We observed a notable decrease in the expression of 47S and 18S rRNAs in D6, albeit without a significant impact on rRNA processing rate (Fig. 2J). In D8, although rDNA transcription and rRNA processing rate restored to normal levels, they did not exhibit the upregulation observed in the early inhibition group (Fig. 2K). Degrading BRD4 solely during the early stage facilitates the inactivation of rDNA transcription, thereby promoting a more immediate and robust reactivation of rDNA transcription during the middle-late stage.

The mechanism by which BRD4 regulates rDNA transcription during iPSC reprogramming

Based on the results presented above, we have discovered that BRD4 plays an important role in regulating rDNA transcription during iPSC reprogramming. We aimed to investigate the underlying mechanism involved. As shown in Fig. 3A–B, immunofluorescence (IF) was conducted to determine the distribution of BRD4 and UBF. While a substantial portion of BRD4 was observed to localize within the nucleoplasm and might primarily function as an elongation protein regulating Pol II pause release [35], a fraction of BRD4 was also found to co-localize with UBF within the nucleolar region. Furthermore, this co-localization between BRD4 and UBF was markedly diminished upon treatment with AT6 on D0 (Fig. 3A–B). Next, co-immunoprecipitation (CO-IP) was performed to confirm the binding between BRD4 and UBF in the process of iPSC reprogramming. As anticipated, BRD4 exhibited strong binding affinity with UBF in the control group (Fig. 3C). The interaction between BRD4 and UBF was disrupted during D2 and D4 due to BRD4 loss and reinstated at D6 upon BRD4 expression restoration (Fig. 3C). To rule out the possibility that the loss of UBF signal observed in AT6 group was due to a decrease in UBF expression, we determined the UBF protein level after treating with AT6, and western-blotting identified that UBF expression was not affected by BRD4 loss (Additional file 1: Fig. S3A). In conclusion, our results confirmed the binding capability of BRD4 to UBF during the iPSC reprogramming process. As is known, UBF localizes the functional rDNA gene unit, which includes the promoter, enhancer, and coding regions [36]. With an enhanced methodology for eliminating background signals in ChIP-seq data, as previously developed in our laboratory (Preprint) [37], we scrutinized the previously reported BRD4 ChIP-seq data (GSE87037) to examine the binding sites of BRD4 in rDNA [38, 39]. By subtracting the non-specific background signal, the signal peak more accurately reflects the enrichment on the genome (Additional file 1: Fig. S3B). In iPSCs, BRD4 was found to localize to the enhancer and promoter of rDNA (Additional file 1: Fig. S3C, upper panel). It is noteworthy that the previously reported public ChIP-seq experiment (GSE193651), in conjunction with prior studies, has delineated the enhancer and promoter regions of rDNA as pivotal target sites for UBF, as illustrated in Additional file 1: Fig. S3C (lower panel) [36, 40, 41]. We here opted to utilize ChIP data from ER-HoxA9 cell lines, an immortalized myeloblast cell lines, in GEO database [42]. ChIP-qPCR was further conducted to ascertain the enrichment of BRD4 and UBF at the rDNA locus during iPSC reprogramming. Here, ChIP-qPCR reveals that BRD4 and UBF truly localize at the promoter and enhancer regions of rDNA during reprogramming (Fig. 3D). Consequently, it demonstrated that both BRD4 and UBF were co-localized at the core promoter and enhancer regions of the

(See figure on next page.)

Fig. 2 Early inhibition of BRD4 accelerates rDNA dynamic expression. **A** Heatmap showing differential gene expression among D0, D2, D4, D6, and D8. Cluster analysis of cell state at indicated times. Differentially expressed genes have|Log2FC|>1 and $P < 0.05$. **B** PCA analysis illustrating the trajectory of reprogramming. **C** Morphology of reprogramming cells at D0 and D4. Red box indicates cells undergoing MET. **D** Dynamic tracking of rDNA expression and rRNA processing rate during reprogramming. **E, F** Western blotting showed BRD4 and pS6 protein expression in the control and D0-AT6 group at indicated day. The bar plot shows statistical results of gray value. **G, H** rDNA expression and rRNA processing rate in control and D0-AT6 group determined by RT-qPCR at D4 and D6, respectively, after BRD4 degradation at D0. **I** Western blotting of S6 in control and D0-AT6 group at D2 and D4, respectively. The bar plot shows statistical results of gray value. **J, K** rDNA expression and rRNA processing rate in control and D4-AT6 group determined by RT-qPCR at D6 and D8, respectively, after BRD4 degradation at D4. All bars represent mean ± SD ($n = 3$ independent experiments; *P <0.05, **P<0.01, ***P <0.001, t test)

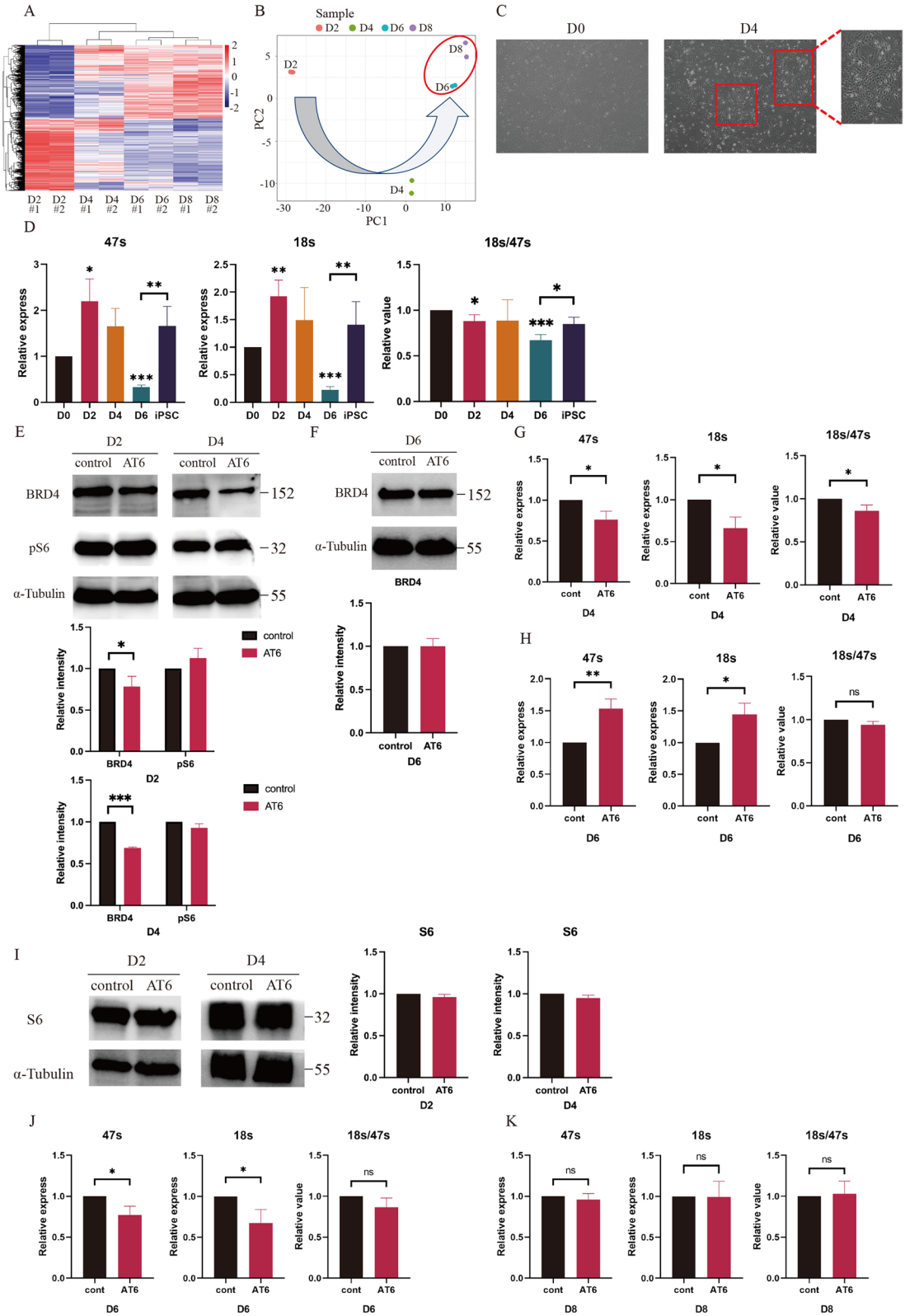

Fig. 2 (See legend on previous page.)

rDNA in the process of iPSC reprogramming (Fig. 3D). Intriguingly, upon AT6 treatment at D0, although BRD4 protein level remained inhibited at D4, the recruitment of BRD4 to the core promoter was restored. Simultaneously, while rDNA expression was still inactive, the enrichment of UBF had been fully reinstated, even showing higher levels (Fig. 3D). This observation gives rise to the hypothesis that the premature re-establishment of BRD4 and UBF on the rDNA locus at D4 might have been preparatory for the subsequent efficient activation of rDNA at D6, notwithstanding the concurrent inactivation of BRD4 expression and inhibition of rDNA transcription during this period. However, further meticulous investigation is imperative to validate this hypothesis thoroughly. In summary, these findings indicate that during iPSC reprogramming, BRD4 binds UBF and co-localizes at the enhancer and promoter regions of rDNA. As UBF is a nucleolar-specific protein containing a high mobility group (HMG), exhibiting DNA-binding activity through its HMG box structure [43–45], we propose that UBF might recruit BRD4 to the enhancer and promoter regions of rDNA.

We further investigated how BRD4 regulated rDNA expression after localizing at rDNA during iPSC reprogramming. After excluding the background signal from previously reported ChIP-seq data of BRD4, H3K27ac, and H3K27me3 in iPSC (GSE87037), we still observed much enrichment signals of BRD4 and H3K27ac, rather than H3K27me3, at both the promoter and enhancer regions of rDNA, though a greater signal density was observed at the upstream region (Additional file 1: Fig. S3D) [38, 39]. Consequently, ChIP-seq data analysis revealed co-localization of BRD4 and H3K27ac, but not H3K27me3, at the enhancer and promoter of iPSC rDNA (Additional file 1: Fig. S3D). This co-localization could be due to two possibilities: (i) BRD4 improves the enrichment of H3K27ac nearby and (ii) BRD4 recognizes and binds the H3K27ac as the reader of acetylation. To validate the true reason, we inhibited BRD4 in D0 and examined the enrichment of H3K27ac at the core promoter and enhancer by ChIP-qPCR at D4. The results not only demonstrated the BRD4 and H3K27ac truly co-locate at the promoter and enhancer of rDNA but also uncovered that the enrichment of H3K27ac at the core promoter and enhancer was significantly decreased upon BRD4 loss (Fig. 3E). Therefore, our findings suggest that during iPSC reprogramming, BRD4 interacts UBF, and co-localizes at the cis-element of rDNA, which in turn facilitates H3K27ac modification nearby to promote rDNA expression.

siRNA interfering Brd4 expression in early stage could also improve reprogramming

To further confirm our conclusions, we employed siRNA to verify the effect of BRD4 loss on early reprogramming. We first confirmed the efficiency of the two siRNA in decreasing Brd4 expression by approximately 50%, which was similar to the effect of AT6 treatment, employing RT-qPCR and western blotting (Additional file 1: Fig. S4A). We evaluated reprogramming efficiency by employing AP staining after interfering with Brd4 expression by two distinct siRNA at D0. We observed early interference by both siRNAs, resulting in improved reprogramming efficiency, consistent with AT6 treatment (Fig. 4A and Additional file 1: Fig. S4B). Meanwhile, the similar increased reprogramming efficiency is also observed upon interfering Brd4 at D2 (Additional file 1: Fig. S4C). Next, we assess both Brd4 transcription and protein expression using RT-qPCR and western blotting at D2 and D4 following D0-siRNA interference (Fig. 4B). We observed that while both Brd4 transcription and protein expression were inactive at D2, the protein expression had been restored at D4 despite Brd4 transcription still being inhibited. Furthermore, we also identified similar rDNA transcription profiles as AT6 experiment. Early interference with Brd4 expression was found to downregulate rDNA transcription more efficiently in the early stage and restore it in the middle-late stage (Fig. 4C). Interestingly, in D4, although 47 s and 18 s were still inhibited upon Brd4 interference, the rRNA processing rate was strongly increased. We hypothesize that the heightened processing rate observed herein may be aimed at salvaging ribosomal function, thereby facilitating more efficient restoration of BRD4 protein translation, notwithstanding the continued inactivity of Brd4 transcription. This positive feedback eventually promotes rDNA restoration via

(See figure on next page.)

Fig. 3 BRD4 colocalize UBF, and regulate rDNA expression via modifying H3K27ac. **A, B** Representative image of immunofluorescence for BRD4 and UBF in D2/D4 control and D2/D4 AT6 group, respectively, after BRD4 inhibition at D0. Scale bar = 10 μm. The bar plot shows the percentage of BRD4-UBF colocalized cell in average of 100 cells ($n = 100$). **C** Temporal change of the interaction between BRD4 and UBF in the control and D0-AT6 groups on D2, D4, and D6. "cont" denotes the group with DMSO at D0, while "AT6" denotes the group treated with AT6 at D0. **D** The ChIP-qPCR analysis unveiled the recruitment of BRD4 and UBF to the core promoter and enhancer regions of rDNA in both the control and D0-AT6 groups at the indicated days. **E** ChIP-qPCR showing the enrichment of H3K27ac at core promoter and enhancer of rDNA in control and D0-AT6 group at D4. All bars represent mean ± SD ($n = 3$ independent experiments; *$P < 0.05$, **$P < 0.01$, ***$P < 0.001$, t test)

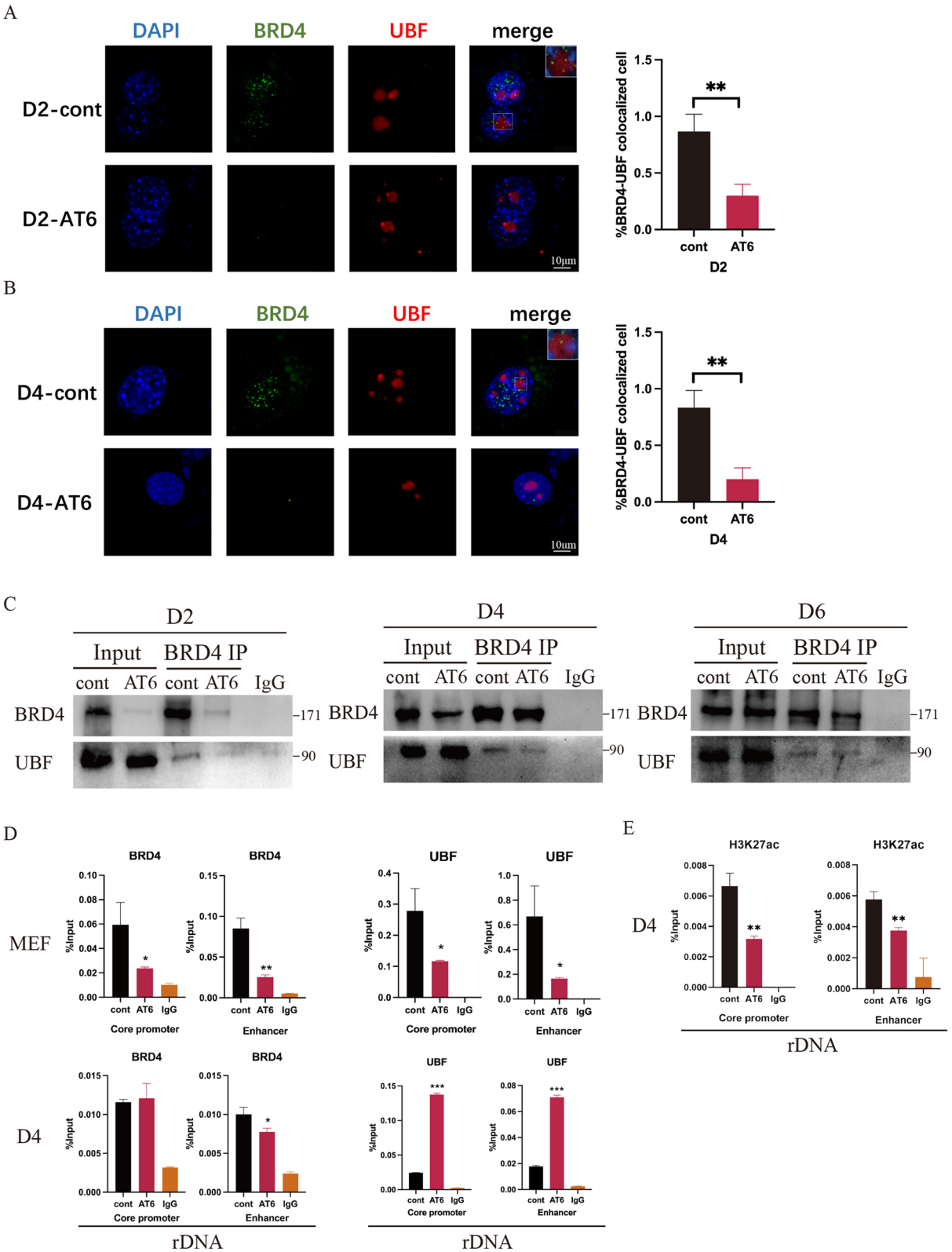

Fig. 3 (See legend on previous page.)

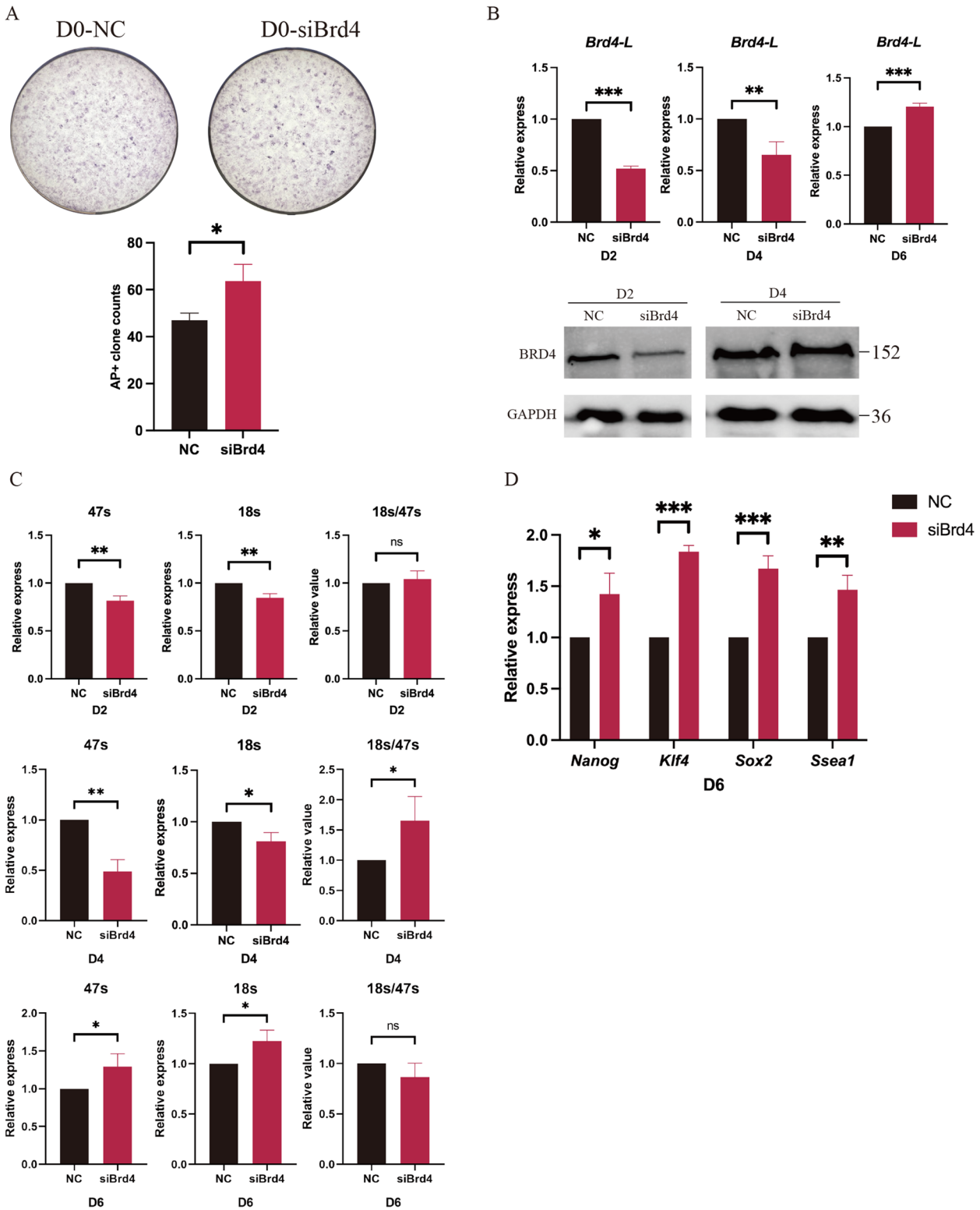

Fig. 4 Early interference of Brd4 improves reprogramming efficiency. **A** AP staining and analysis of reprogramming efficiency in NC and D0-siBrd4 #1 group. The bar plot presents the AP+ clone counts.**B** Brd4/BRD4 mRNA and protein expression detected by RT-qPCR (upper) and western-blotting (lower) in NC and siBrd4 #1 group at indicated days after Brd4 interference at D0. **C** rDNA expression and rRNA processing rate at indicated times after Brd4 interference (siBrd4 #1) at D0. **D** mRNA expression levels of pluripotent genes in control and D0-siBrd4 #1 group at D6. All bars represent mean ± SD ($n = 3$ independent experiments; *$P < 0.05$, **$P < 0.01$, ***$P < 0.001$, *t* test)

raised BRD4 levels. Additionally, we also found an activation in pluripotent gene expression at middle-late stage after interfering with Brd4 expression in the early stage (Fig. 4D). These findings suggest that early inhibition of BRD4 definitely improves iPSC reprogramming, possibly through facilitating sequential and dynamic alterations in rDNA.

Inhibition of BRD4 in the early stage promotes exit of cells from the somatic state

In the process of iPSC reprogramming, erasing somatic identity in the early stage is of paramount importance [6, 7, 46]. Our studies have demonstrated that early inhibition of BRD4 was sufficient to activate pluripotent genes, but it is still unclear if it could facilitate somatic identity erasing. Previous research has provided evidence that interference with somatic gene transcription through the inhibition of the BET protein family using JQ1 can effectively enhance the process of reprogramming [29]. Therefore, we hypothesized that degrading BRD4 in the early stage might promote cells to exit the somatic state. To test this hypothesis, we screened a series of somatic-related genes that were specifically downregulated in the early stage. Figure 5A shows the working schedule briefly (Fig. 5A). First of all, three independent RNA-seq data from GEO datasets were reanalyzed to identify downregulated genes throughout the reprogramming process using differential expression analysis (GSE70022, GSE46104, GSE156437) [27, 28, 47–50]. GO analysis was then conducted on the downregulated genes, and a total of 293 somatic genes common in three datasets were identified (Fig. 5B). Subsequently, 233, 165, and 95 somatic genes, which must be downregulated in the early stages of reprogramming, were identified from GSE70022, GSE113430, and GSE138817, respectively (Fig. 5C) [27, 28, 51–54]. By overlapping these genes, 73 somatic genes were successfully identified as somatic genes specifically downregulated in the early stage (Fig. 5D). Consequently, we classified these 73 genes as crucial candidates for early-stage inactivation during iPSC reprogramming. We chose the top five genes and validated their expression in our reprogramming system using RT-qPCR (Fig. 5E). Apart from Emilin, all somatic genes were conspicuously downregulated in the early stage. However, although Emilin was not significantly downregulated, it still showed a decreasing trend (Fig. 5E). Moreover, the expression of all somatic genes was notably decreased in the early stage upon BRD4 loss by AT6 treatment or siRNA in D0 (Fig. 5F and Additional file 1: Fig. S4D). In conclusion, the early inhibition of BRD4 substantially decreases the expression of somatic-related genes, potentially inducing cells to depart from the somatic state and expedite the transition towards pluripotency.

Discussion

The transcription of rDNA, which is essential for cellular ribosomal biogenesis, is associated with protein synthesis and imposes limitations on cellular proliferation [55, 56]. During the conversion of differentiated MEFs into pluripotent iPSCs, the activation of silent rDNA is a critical event. Our study unveiled a transient surge, succeeded by a gradual decline, and ultimately, the restoration of rDNA transcription during iPSC reprogramming, consistent with previous reports, emphasizing the dynamic nature of rDNA expression during this process [24]. Several studies have shown that the efficiency of reprogramming, whether through SCNT or iPSC reprogramming, is correlated with rDNA transcription [24, 25, 34, 57]. BRD4, a member of the BET protein family, is involved in the regulation of gene expression through various mechanisms [58]. It plays diverse roles in gene transcription, embryonic development, cell cycle regulation, and tumorigenesis [13, 59–61]. The functionality of the BET protein family has been elucidated in iPSC reprogramming, revealing that a deficiency in the early stage can enhance reprogramming efficiency by suppressing the expression of somatic genes. Nevertheless, the specific BET family member accountable for this phenomenon has yet to be identified [29]. Therefore, it is imperative to delve into the intricate functions of these members throughout the iPSC reprogramming process. Recent studies have elucidated the involvement of BRD4 in the modulation of iPSC reprogramming, primarily through the activation of pluripotency-associated genes during the middle-late stages [17]. Additionally, BRD4 has been shown to augment rDNA transcription by facilitating the acetylation of histone H3 and H4 in 293 T cells

(See figure on next page.)

Fig. 5 Early inhibition of BRD4 reduces expression of somatic-related genes. **A** Flowchart outlining the steps of this part. **B** Differential expression analysis and GO enrichment analysis between D0 and iPSC. **C** Differential expression analysis of somatic genes from **B** between D0 and D3/D4 group. **D** Venn diagram showing the overlap of somatic genes that need to be turned off in the early stage from three datasets. **E** RT-qPCR determined the mRNA expression levels of genes from **D**. **F** mRNA expression levels of somatic genes in control and D0-AT6 group at D4. All bars represent mean ± SD ($n = 3$ independent experiments; *$P<0.05$, **$P<0.01$, ***$P < 0.001$, t test). Differentially expressed genes have |Log2FC|>1 and $P < 0.05$

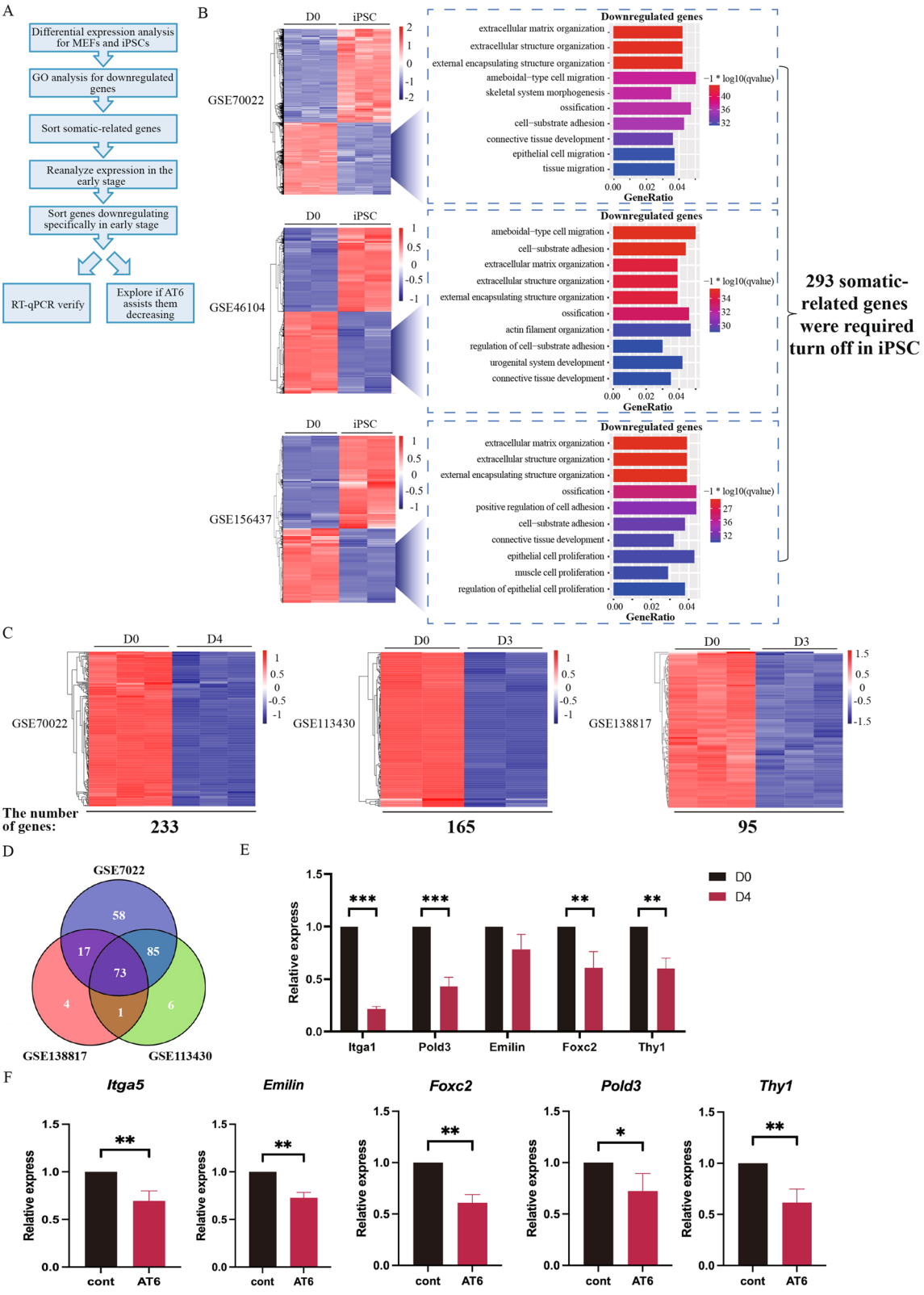

Fig. 5 (See legend on previous page.)

[19]. Consequently, an intriguing inquiry arises regarding the potential impact of BRD4 on iPSC reprogramming, not only through the activation of pluripotency genes as previously documented but also via the regulation of dynamic changes in rDNA expression. In this study, we conducted early inhibition of BRD4 using AT6 or siRNA, which not only immediately reduced rDNA transcription but also efficiently restored it, thereby enhancing iPSC reprogramming. These findings imply that the BRD4-mediated dynamic regulation of rDNA transcription carries substantial implications for the process of iPSC reprogramming. Moreover, it reminds that additional factors governing rDNA transcription may also regulate iPSC reprogramming.

Our study has shed light on the mechanism by which BRD4 governs rDNA transcription during iPSC reprogramming. Based on prior investigations, UBF, a nucleolar-specific HMG-box-containing protein, has been identified as capable of binding to DNA via its HMG box, thereby facilitating the assembly of the pre-initiation complex (PIC) at the rDNA promoter [43–45]. Recent evidence has elucidated that LYAR is mobilized by UBF to bind to rDNA in 293 T cells, subsequently facilitating the recruitment of BRD4 to modulate rDNA transcription [19]. Consistent with these findings, our study also demonstrates the interaction and co-localization between BRD4 and UBF during the mouse iPSC reprogramming. Consequently, we imply that throughout iPSC reprogramming, UBF recruits BRD4 to the promoter and enhancer regions of rDNA. BRD4 further regulates rDNA transcription by modulating the levels of H3K27ac in the vicinity, thus impacting rDNA expression. However, the co-localization between BRD4 and H3K27ac at the rDNA locus observed in our study also suggests that BRD4's localization to rDNA may involve not only its interaction with UBF but also its bromodomain, which functions as an acetylation reader [62]. Conducting detailed structural analyses of BRD4 will not only advance our understanding of its molecular characteristics but also provide crucial insights into the complete mechanism of rDNA transcription during iPSC reprogramming. Moreover, considering the genomic localization of BRD4 and its role as a scaffold for recruiting diverse transcription factors during mRNA transcription, future research investigating whether BRD4 acts as a scaffold for recruiting known and unknown transcription factors to influence rDNA expression and impact iPSC reprogramming would be of great value.

iPSC reprogramming has emerged as a powerful biological tool with tremendous potential in various fields. However, numerous obstacles impede its application, with the ambiguous understanding of the underlying biological processes being a major challenge. Hence, it is valuable to elucidate the mechanisms governing these processes. In our study, we have concluded that early depletion of BRD4 markedly improves iPSC reprogramming by immediately inactivating a series of somatic genes and activating pluripotency-associated genes. Conversely, inhibiting BRD4 during the middle-late stage severely impedes reprogramming, resulting in a failure to activate pluripotency-associated genes, consistent with previous studies [17]. Thus, our findings indicate that BRD4 plays a dual role during iPSC reprogramming, acting as a negative factor in the early stage but a positive factor in the middle-late stage. This study expands our current knowledge regarding the involvement of BRD4 in iPSC reprogramming and fills a gap in our understanding of the early-stage function of BRD4 in reprogramming. In the future, it would be worth investigating whether BRD4 is also involved in the late-stage reorganization of chromatin structure.

With the advancement of iPSC reprogramming, there is growing evidence suggesting a significant resemblance between iPSC reprogramming and tumorigenesis [63]. Notably, one of the prominent shared features between these processes is the alteration of rDNA transcription. Previous studies have demonstrated the activation of a substantial number of rDNA transcriptions in both iPSC reprogramming and tumorigenesis [64]. Therefore, in various tumor diseases, early inhibition of BRD4 may also exacerbate tumorigenesis. Given that BRD4 inhibitors have been identified to play pivotal roles in clinical tumor treatment [65], it hence bears significant scientific merit to explore whether premature inhibition of BRD4 would lead to hastened dynamic expression of rDNA and potentially promote tumorigenesis during clinical intervention. In conclusion, it is imperative to investigate this issue, as it would significantly advance our understanding of the potential adverse effects associated with BRD4 inhibitors.

Conclusions

In this study, we observed a noteworthy enhancement in iPSC reprogramming through early inhibition of BRD4, characterized by the facilitation of modulation in rDNA expression dynamics. The early degradation of BRD4 efficiently facilitates the inactivation of rDNA in the early stage, which is subsequently restored in the middle-late stage. During iPSC reprogramming, BRD4 has been observed to interact with UBF and co-localize at the promoter and enhancer regions of rDNA. Additionally, BRD4 has been shown to facilitate the H3K27ac levels in the surrounding vicinity, consequently regulating rDNA expression. Moreover, early inhibition of BRD4 effectively suppresses somatic gene expression and activated pluripotent gene transcription. Our findings indicate that

BRD4 acts as a negative regulator in the early stage of iPSC reprogramming, while it remains indispensable in the middle-late stage.

Methods

Reagents

The following antibodies and dilutions were used for western blotting and immunofluorescence: BRD4 rabbit mAb (ab128874, Abcam) at 1/1000 for WB and 1/100 for IF, UBF mouse mAb (sc-13125, Santa Cruz Biotechnology) at 1/1000 for WB and 1/50 for IF, S6 rabbit mAb (#2217, CST) at 1/1000 for WB, P-S6 rabbit mAb (#4858, CST) at 1/1000 for WB, α-Tubulin pAb (11,224–1-AP, Proteintech) at 1/2000 for WB, AFP mouse mAb (sc-130302, Santa Cruz Biotechnology) at 1/50 for IF, α-sma rabbit pAb (14,395–1-AP, Proteintech) at 1/100 for IF, and nestin goat pAb (sc-21248, Santa Cruz Biotechnology) at 1/50 for IF. For co-immunoprecipitation, the antibody used was BRD4 rabbit mAb (ab243862, Abcam) at 7 μl/0.5 mg lysate. For ChIP-qPCR, the antibody used was H3K27ac rabbit mAb (#8173S, CST) at a dilution of 1:100. The specific BRD4 degradation agent used was AT6 (HY-112375, MCE).

Mice and cell culture

We obtained female C57BL/6 and male DBA/2 mice from Vital River (Beijing, China) and female and male 4F2A mice from JAX company. To prepare mouse embryonic fibroblasts (MEFs), we obtained E13.5 male homozygous embryos from B6D2F1 and 4F2A mice. MEFs and 293 T cells used in experiments were cultured in Dulbecco's modified Eagle medium (DMEM) supplemented with 15% fetal bovine serum (FBS, Gibco), 1% MEM non-essential amino acids (NEAA, Gibco), 1% L-glutamine (Gibco), and 1% penicillin–streptomycin (Biological Industries). 4F2A MEFs used in iPSC reprogramming were cultured in knockout DMEM (KO-DMEM, Gibco) containing 15% knockout serum replacement (KOSR, Gibco), 1% MEM NEAA, 1% L-glutamine, 1% penicillin–streptomycin, 1% sodium pyruvate (Gibco), 1000 U/mL LIF, 0.1% 2-mercaptoethanol, and 2 μg/mL doxycycline. For embryoid bodies, we used KO-DMEM, 15% KOSR, 1% MEM NEAA, 1% L-glutamine, 1% penicillin–streptomycin, and 1% sodium pyruvate.

iPSC generation

To establish the virus-induced pluripotent stem cell (iPSC) reprogramming system, 293 T cells were transfected with Teton-OSKM and viral packaging plasmids (PSPAX, PMD2G, and rtTA) using Lipofectamine 3000 transfection reagent (Invitrogen). After a 6-h incubation in Opti-MEM Reduced-Serum Medium (without antibiotics), the medium was replaced with MEF medium and cultured for 48 h. The harvested supernatants containing the retroviruses were used to infect MEFs along with 5 μg/ml polybrene, followed by reseeding on mitomycin C-treated MEF feeder layers. The MEFs were then cultured in MEF medium supplemented with 2 μg/mL doxycycline for 3 days and subsequently in iPSC medium containing 2 μg/mL doxycycline until reprogramming was completed. The medium was refreshed daily.

To initiate 4F2A iPSC reprogramming, mitomycin C-treated MEF feeder layers were prepared in 6-well plates or 10-cm dishes, and 4F2A MEFs were seeded onto them. The cells were cultured in MEF medium supplemented with 2 μg/mL doxycycline for 3 days. The medium was then replaced with iPSC medium containing 2 μg/mL doxycycline. The fresh medium was provided daily.

To treat reprogramming cells with AT6, the cells were cultured in medium supplemented with AT6 solution, which was dissolved in DMSO, at the specified time. For Brd4 interference experiments, siRNA duplexes of si-NC and si-Brd4 were transfected into control and siBrd4 MEFs using lipofectamine 3000 transfection reagent at the indicated time. During the treatment period, the culture medium containing AT6 was refreshed daily. Following the completion of treatment, we transitioned to cultivating the cells in normal medium of MEF or iPSC, with daily medium changes maintained until the designated time point for examination.

Embryoid body (EB) differentiation assay

The iPSCs were initially digested using an adequate amount of trypsin/EDTA until cell detachment. To neutralize the trypsin, twice the volume of MEF medium relative to trypsin was added. The cells were then centrifuged at 1000 rpm for 5 min and subsequently resuspended to achieve a single-cell suspension. Approximately 5×10^5 iPSCs were replated in 8 ml of medium onto low-attachment plates. Embryoid bodies were cultured in knockout DMEM, supplemented with 15% knockout serum replacement, 1% MEM non-essential amino acids (NEAA), 1% L-glutamine, and 1% penicillin–streptomycin, under conditions of 37 °C and 5% CO2 for 1 week before transitioning to MEF medium. The culture medium was replenished every 3 days.

Western-blot

The western blotting experiments were performed using a previously established protocol [24]. After transfer, polyvinylidene fluoride (PVDF) membranes were blocked with 0.1% PBS-Tween (PBS-T) containing 5% milk for 1 h at room temperature. The membranes were then incubated with primary antibody solution overnight at 4 °C. Antibody binding was detected using specific secondary

antibodies. The quantification of blots was performed using ImageJ analysis software.

Immunofluorescence

The cells were fixed by incubating them with 4% paraformaldehyde (PFA) for 30 min at room temperature, followed by permeabilization with 0.25% PBS-T for 20 min. After blocking with 1% BSA for 30 min, the cells were incubated with the primary antibody at 4℃ overnight. The cells were then washed three times with PBST and incubated with the secondary antibody for 1 h at room temperature. After washing with PBS-T three times, the cells were incubated with DAPI for 5 min. Finally, the slides were observed using a Nikon ECLIPSE Ti-U microscope.

Co-immunoprecipitation

The cells were lysed in NP-40 Lysis Buffer (Beyotime) and incubated with 0.5–2 μg of the antibody or control rabbit IgG at 4℃ overnight. Immunoprecipitation was performed using the Pierce™ Classic Magnetic IP/Co-IP Kit (Thermo Fisher) as per the manufacturer's instructions, followed by Western blot analysis.

Alkaline phosphatase staining and staining-positive colony counting

The BCIP/NBT alkaline phosphatase colour development kit (Beyotime) was used to perform alkaline phosphatase (AP) staining following the manufacturer's instructions. The number of AP-positive colonies was determined using ImageJ analysis software.

RNA extraction and RT-qPCR

The total RNA was extracted using the RNAeasy™ Animal RNA Isolation Kit with Spin Column (Beyotime) following the manufacturer's protocol. Subsequently, cDNA was synthesized from RNA using the TransScript All-in-One First-Strand cDNA Synthesis SuperMix for qPCR (One-Step gDNA Removal) kit. RT-qPCR was performed as previously described [24]. The list of primers used in this study is provided in the Additional file 2.

Analysis of rDNA in ChIP-seq and background subtraction

The analysis procedures were performed according to a previous report [37]. Raw data were obtained from NCBI-GEO databases and subjected to quality control using FastQC. Trimmomatic was used to remove adapter sequences and filter out low-quality reads. The data was then aligned to the mouse rDNA repeat (GenBank BK000964.3) using Bowtie2 (version 2.3.5.1) and converted and sorted using SAMtools (version 1.3.1). The normalization factor, r, was calculated using NCIS, and the background of the ChIP-seq data was subtracted using Python scripts for "background subtraction". The detailed process of "background subtraction" was performed as previously described [37]. The visualization of ChIP-seq data was performed using IGV.

RNA-seq analysis

The raw data were obtained from NCBI-GEO databases and subjected to quality checking using FastQC. RNA-seq reads were then aligned to the mouse genome version mm10 using hisat2 (version 2.2.1). The resulting alignments were converted and sorted using SAMtools, and featureCounts (version 2.0.3) was used to determine expression levels. Subsequent bioinformatics analyses were performed using R programming language (version 4.1.0). The DE analysis was conducted using the R package DESeq2. The GOplot package was used to generate the relevant plots.

ChIP-qPCR

The ChIP-qPCR experiment was conducted according to the manufacturer's instructions of the SimpleChIP® Enzymatic Chromatin IP Kit (Magnetic Beads) (CST, #9003). Initially, 1% paraformaldehyde was used to crosslink reprogramming cells for 10 min at room temperature, followed by glycine quenching for 5 min to terminate the crosslinking reaction. After isolating the nuclei, the nuclear fraction was digested with MNase. The solubilized chromatin was subsequently incubated with antibodies against the related proteins or IgG overnight at 4℃. A 2% sample of the mixture was collected as input. The ChIP-Grade Protein G Magnetic Beads were incubated with the mixtures for 2 h at 4℃. The chromatin-antibody complex was isolated and washed, and the immunoprecipitated DNA was purified after crosslink reversal. Finally, the purified DNA fragments were quantified by RT-qPCR using the ChIP-qPCR primers listed in Additional file 2.

Statistical analyses

All experiments were conducted independently in triplicate. Results are presented as mean ± standard deviation (SD) for statistical comparison. Statistical significance was determined using Student's unpaired two-tailed *t*-test with GraphPad Prism 5 (GraphPad), where $p < 0.05$, 0.01, and 0.001 were denoted as (*), (**), and (***), respectively.

Abbreviations

AP	Alkaline phosphatase
ALS	Amyotrophic lateral sclerosis
BET	Bromodomain and extra-terminal
CCK8	Cell Counting Kit-8
CIN	Cervical intraepithelial neoplasia
ESC	Embryonic stem cells
FTD	Frontotemporal dementia

HCC	Human hepatocellular carcinoma
HD	Huntington's disease
HMG	High mobility group
iPSC	Induced pluripotent stem cells
LIF	Leukemia inhibitory factor
MEFs	Mouse embryo fibroblasts
MET	Mesenchymal-epithelial transition
PCA	Principal component analysis
PIC	Pre-initiation complex
Pol II	RNA polymerase II
pS6	Phospho-S6 ribosomal protein
P-TEFb	Positive transcription elongation factor b
rDNA	Ribosomal DNA
S6	S6 ribosomal protein
SCNT	Somatic cell nuclear transfer
SE	Super enhancer
UBF	Upstream binding factor 1

Supplementary Information

The online version contains supplementary material available at https://doi.org/10.1186/s12915-024-01997-9.

Additional file 1: Figure S1-S4. FigS1- Reprogramming efficiency is diverse when degrading BRD4 in different days. FigS2- Early inhibition of BRD4 accelerates rDNA dynamic expression. FigS3- BRD4 associates with UBF to localize at rDNA, thereby enhancing H3K27ac levels in the vicinity to regulate rDNA transcription. FigS4- Early interfering Brd4 improves reprogramming efficiency via siRNA.

Additional file 2: Primers information and data accession.

Additional file 3: Original western blotting images.

Acknowledgements
Not applicable

Authors' contributions
ZZ: Conception and design of the experiment, performed the experiment, data analysis and interpretation, and manuscript writing. XH: Performed the experiment. YS: Performed the experiment. LL: Conception and design of the experiment, financial support, administrative support, and manuscript writing. ZL: Financial support and administrative support. All authors read and approved the final manuscript.

Funding
This work was supported by the following projects: National Natural Science Foundation of China (no. 32272885) and the Key projects of Heilongjiang Natural Science Foundation (no. ZD2021C005).

Availability of data and materials
The ChIP-seq and RNA-seq data that corroborate the conclusions presented in this manuscript can be accessed through the NCBI-GEO at https://www.ncbi.nlm.nih.gov/geo/. The accession numbers for the related data that were utilized in this study are listed in Additional file 2.

Declarations

Ethics approval and consent to participate
All animal experiments were implemented in line with the Guidelines for Animal Experiments of Harbin Medical University (HMUIRB20190011).

Competing interests
The authors declare that there is no conflict of interest.

Consent for publication
Not applicable.

Received: 5 March 2024 Accepted: 28 August 2024
Published online: 11 September 2024

References

1. Takahashi K, Yamanaka S. Induction of pluripotent stem cells from mouse embryonic and adult fibroblast cultures by defined factors. Cell. 2006;126(4):663–76
2. Rodriguez-Osorio N, Urrego R, Cibelli JB, Eilertsen K, Memili E. Reprogramming mammalian somatic cells. Theriogenology. 2012;78(9):1869–86.
3. Li D, Liu J, Yang X, Zhou C, Guo J, Wu C, et al. Chromatin accessibility dynamics during iPSC reprogramming. Cell Stem Cell. 2017;21(6):819–33 e6.
4. Knaupp AS, Buckberry S, Pflueger J, Lim SM, Ford E, Larcombe MR, et al. Transient and permanent reconfiguration of chromatin and transcription factor occupancy drive reprogramming. Cell Stem Cell. 2017;21(6):834–45 e6.
5. Chen J, Chen X, Li M, Liu X, Gao Y, Kou X, et al. Hierarchical Oct4 binding in concert with primed epigenetic rearrangements during somatic cell reprogramming. Cell Rep. 2016;14(6):1540–54.
6. Polo JM, Anderssen E, Walsh RM, Schwarz BA, Nefzger CM, Lim SM, et al. A molecular roadmap of reprogramming somatic cells into iPS cells. Cell. 2012;151(7):1617–32.
7. Li R, Liang J, Ni S, Zhou T, Qing X, Li H, et al. A mesenchymal-to-epithelial transition initiates and is required for the nuclear reprogramming of mouse fibroblasts. Cell Stem Cell. 2010;7(1):51–63.
8. Wei Z, Gao F, Kim S, Yang H, Lyu J, An W, et al. Klf4 organizes long-range chromosomal interactions with the oct4 locus in reprogramming and pluripotency. Cell Stem Cell. 2013;13(1):36–47.
9. Apostolou E, Ferrari F, Walsh RM, Bar-Nur O, Stadtfeld M, Cheloufi S, et al. Genome-wide chromatin interactions of the Nanog locus in pluripotency, differentiation, and reprogramming. Cell Stem Cell. 2013;12(6):699–712.
10. Apostolou E, Stadtfeld M. Cellular trajectories and molecular mechanisms of iPSC reprogramming. Curr Opin Genet Dev. 2018;52:77–85.
11. de Wit E, Bouwman BA, Zhu Y, Klous P, Splinter E, Verstegen MJ, et al. The pluripotent genome in three dimensions is shaped around pluripotency factors. Nature. 2013;501(7466):227–31.
12. Denholtz M, Bonora G, Chronis C, Splinter E, de Laat W, Ernst J, et al. Long-range chromatin contacts in embryonic stem cells reveal a role for pluripotency factors and polycomb proteins in genome organization. Cell Stem Cell. 2013;13(5):602–16.
13. Liu W, Stein P, Cheng X, Yang W, Shao NY, Morrisey EE, et al. BRD4 regulates Nanog expression in mouse embryonic stem cells and preimplantation embryos. Cell Death Differ. 2014;21(12):1950–60.
14. Arnold M, Bressin A, Jasnovidova O, Meierhofer D, Mayer A. A BRD4-mediated elongation control point primes transcribing RNA polymerase II for 3'-processing and termination. Mol Cell. 2021;81(17):3589-60 e13.
15. Jang MK, Mochizuki K, Zhou M, Jeong HS, Brady JN, Ozato K. The bromodomain protein Brd4 is a positive regulatory component of P-TEFb and stimulates RNA polymerase II-dependent transcription. Mol Cell. 2005;19(4):523–34.
16. Yang Z, Yik JH, Chen R, He N, Jang MK, Ozato K, et al. Recruitment of P-TEFb for stimulation of transcriptional elongation by the bromodomain protein Brd4. Mol Cell. 2005;19(4):535–45.
17. Liu L, Xu Y, He M, Zhang M, Cui F, Lu L, et al. Transcriptional pause release is a rate-limiting step for somatic cell reprogramming. Cell Stem Cell. 2014;15(5):574–88.
18. Di Stefano B, Collombet S, Jakobsen JS, Wierer M, Sardina JL, Lackner A, et al. C/EBPalpha creates elite cells for iPSC reprogramming by upregulating Klf4 and increasing the levels of Lsd1 and Brd4. Nat Cell Biol. 2016;18(4):371–81.
19. Izumikawa K, Ishikawa H, Yoshikawa H, Fujiyama S, Watanabe A, Aburatani H, et al. LYAR potentiates rRNA synthesis by recruiting BRD2/4 and the MYST-type acetyltransferase KAT7 to rDNA. Nucleic Acids Res. 2019;47(19):10357–72.
20. Sun Y, Hu X, Qiu D, Zhang Z, Lei L. rDNA Transcription in Developmental Diseases and Stem Cells. Stem Cell Rev Rep. 2023;19(4):839–52.

21. Kim DS, Camacho CV, Nagari A, Malladi VS, Challa S, Kraus WL. Activation of PARP-1 by snoRNAs controls ribosome biogenesis and cell growth via the RNA helicase DDX21. Mol Cell. 2019;75(6):1270–85 e14.
22. Hannan AJ. Tandem repeats mediating genetic plasticity in health and disease. Nat Rev Genet. 2018;19(5):286–98.
23. Kim HG, Huot JR, Pin F, Guo B, Bonetto A, Nader GA. Reduced rDNA transcription diminishes skeletal muscle ribosomal capacity and protein synthesis in cancer cachexia. FASEB J. 2021;35(2): e21335.
24. Zhao Q, Wu Y, Shan Z, Bai G, Wang Z, Hu J, et al. Serum starvation-induced cell cycle synchronization stimulated mouse rDNA transcription reactivation during somatic cell reprogramming into iPSCs. Stem Cell Res Ther. 2016;7(1):112.
25. Liao C, Pang N, Liu Z, Lei L. Transient inhibition of rDNA transcription in donor cells improves ribosome biogenesis and preimplantation development of embryos derived from somatic cell nuclear transfer. FASEB J. 2020;34(6):8283–95.
26. Shi J, Zhang Y, Tan D, Zhang X, Yan M, Zhang Y, et al. PANDORA-seq expands the repertoire of regulatory small RNAs by overcoming RNA modifications. Nat Cell Biol. 2021;23(4):424–36.
27. Xing Y, Carstens R. Multiphasic and dynamic changes in alternative splicing during induction of pluripotency are coordinated by numerous RNA binding proteins [iPS]. In.: GEO: https://www.ncbi.nlm.nih.gov/geo/query/acc.cgi?acc=GSE70022; 15 Mar 2016.
28. Cieply B, Park JW, Nakauka-Ddamba A, Bebee TW, Guo Y, Shang X, et al. Multiphasic and dynamic changes in alternative splicing during induction of pluripotency are coordinated by numerous RNA-binding proteins. Cell Rep. 2016;15(2):247–55.
29. Shao Z, Yao C, Khodadadi-Jamayran A, Xu W, Townes TM, Crowley MR, et al. Reprogramming by de-bookmarking the somatic transcriptional program through targeting of BET bromodomains. Cell Rep. 2016;16(12):3138–45.
30. Gadd MS, Testa A, Lucas X, Chan KH, Chen W, Lamont DJ, et al. Structural basis of PROTAC cooperative recognition for selective protein degradation. Nat Chem Biol. 2017;13(5):514–21.
31. Sun Y, Hu X, Lei L. Different stage of iPSC reprogramming. In.: GEO: https://www.ncbi.nlm.nih.gov/geo/query/acc.cgi?acc=GSE227745; 29 Jul 2024.
32. Velychko S, Adachi K, Kim KP, Hou Y, MacCarthy CM, Wu G, et al. Excluding Oct4 from Yamanaka cocktail unleashes the developmental potential of iPSCs. Cell Stem Cell. 2019;25(6):737–53 e4.
33. Hu X, Huang X, Yang Y, Sun Y, Zhao Y, Zhang Z, et al. Dux activates metabolism-lactylation-MET network during early iPSC reprogramming with Brg1 as the histone lactylation reader. Nucleic Acids Res. 2024;52(10):5529–48.
34. Zheng Z, Jia JL, Bou G, Hu LL, Wang ZD, Shen XH, et al. rRNA genes are not fully activated in mouse somatic cell nuclear transfer embryos. J Biol Chem. 2012;287(24):19949–60.
35. Itzen F, Greifenberg AK, Bosken CA, Geyer M. Brd4 activates P-TEFb for RNA polymerase II CTD phosphorylation. Nucleic Acids Res. 2014;42(12):7577–90.
36. Herdman C, Mars JC, Stefanovsky VY, Tremblay MG, Sabourin-Felix M, Lindsay H, et al. A unique enhancer boundary complex on the mouse ribosomal RNA genes persists after loss of Rrn3 or UBF and the inactivation of RNA polymerase I transcription. PLoS Genet. 2017;13(7): e1006899.
37. Cheng X, Jiang Q, Hu X, Huang X, Hui L, Wei Y, et al. The loss of ATRX/DAXX complex disturbs rDNA heterochromatinization and promotes development of glioma (Preprint). bioRxiv. 2019. https://doi.org/10.1101/745307.
38. Aldiri I, Xu B, Wang L, Chen X, Hiler D, Griffiths L, et al. The dynamic epigenetic landscape of the retina during development, reprogramming, and tumorigenesis. Neuron. 2017;94(3):550–68 e10.
39. Aldiri I, Xu B, Wang L, Chen X, Hiler D, Griffiths L, et al. The dynamic epigenetic landscape of the retina during development, reprogramming, and tumorigenesis [ChIP-Seq_Mm]. In.: https://www.ncbi.nlm.nih.gov/geo/query/acc.cgi?acc=GSE87037; 03 May 2017.
40. Antony C, George SS, Blum J, Somers P, Thorsheim CL, Wu-Corts DJ, et al. Control of ribosomal RNA synthesis by hematopoietic transcription factors. Mol Cell. 2022;82(20):3826–39 e9.
41. Vikram R, Paralkar. Hematopoietic transcription factors bind rDNA and regulate rRNA transcription. In.: GEO: https://www.ncbi.nlm.nih.gov/geo/query/acc.cgi?acc=GSE193651; 15 Jan 2022.
42. Sykes DB, Kfoury YS, Mercier FE, Wawer MJ, Law JM, Haynes MK, et al. Inhibition of dihydroorotate dehydrogenase overcomes differentiation blockade in acute myeloid leukemia. Cell. 2016;167(1):171–86 e15.
43. Stefanovsky VY, Pelletier G, Bazett-Jones DP, Crane-Robinson C, Moss T. DNA looping in the RNA polymerase I enhancesome is the result of non-cooperative in-phase bending by two UBF molecules. Nucleic Acids Res. 2001;29(15):3241–7.
44. Sanij E, Hannan RD. The role of UBF in regulating the structure and dynamics of transcriptionally active rDNA chromatin. Epigenetics. 2009;4(6):374–82.
45. Putnam CD, Copenhaver GP, Denton ML, Pikaard CS. The RNA polymerase I transactivator upstream binding factor requires its dimerization domain and high-mobility-group (HMG) box 1 to bend, wrap, and positively supercoil enhancer DNA. Mol Cell Biol. 1994;14(10):6476–88.
46. Stadtfeld M, Maherali N, Breault DT, Hochedlinger K. Defining molecular cornerstones during fibroblast to iPS cell reprogramming in mouse. Cell Stem Cell. 2008;2(3):230–40.
47. Brady JJ, Li M, Suthram S, Jiang H, Wong WH, Blau HM. Early role for IL-6 signalling during generation of induced pluripotent stem cells revealed by heterokaryon RNA-Seq. Nat Cell Biol. 2013;15(10):1244–52.
48. Liu J, Gao M, Xu S, Chen Y, Wu K, Liu H, et al. YTHDF2/3 are required for somatic reprogramming through different RNA deadenylation pathways. Cell Rep. 2020;32(10): 108120.
49. Liu J. YTHDF2/3 are required for somatic reprogramming through different RNA deadenylation pathways. In.: GEO: https://www.ncbi.nlm.nih.gov/geo/query/acc.cgi?acc=GSE156437; 19 Aug 2020.
50. Brady J, Blau H. Global transcriptome profiling of Oct4/Klf4/Sox2 (3Factor, 3F) + IL6 iPS clones derived from mouse embryonic fibroblasts. In.: GEO: https://www.ncbi.nlm.nih.gov/geo/query/acc.cgi?acc=GSE46104; 28 Aug 2013.
51. Jiang Q, Huang X, Hu X, Shan Z, Wu Y, Wu G, et al. Histone demethylase KDM6A promotes somatic cell reprogramming by epigenetically regulating the PTEN and IL-6 signal pathways. Stem Cells. 2020;38(8):960–72.
52. Di Giammartino DC, Kloetgen A, Polyzos A, Liu Y, Kim D, Murphy D, et al. KLF4 is involved in the organization and regulation of pluripotency-associated three-dimensional enhancer networks. Nat Cell Biol. 2019;21(10):1179–90.
53. Apostolou E, Tsirigos A. KLF4 binding is involved in the organization and regulation of 3D enhancer networks during acquisition and maintenance of pluripotency [RNA-seq]. In.: GEO: https://www.ncbi.nlm.nih.gov/geo/query/acc.cgi?acc=GSE113430; 6 Sep 2019.
54. Qi J. Histone demethylase KDM6A promotes somatic cell reprogramming by epigenetically regulate PTEN and IL-6 signal pathway; In.: GEO: https://www.ncbi.nlm.nih.gov/geo/query/acc.cgi?acc=GSE138817; 20 Oct 2021.
55. Kopp K, Gasiorowski JZ, Chen D, Gilmore R, Norton JT, Wang C, et al. Pol I transcription and pre-rRNA processing are coordinated in a transcription-dependent manner in mammalian cells. Mol Biol Cell. 2007;18(2):394–403.
56. Condon C, Squires C, Squires CL. Control of rRNA transcription in Escherichia coli. Microbiol Rev. 1995;59(4):623–45.
57. Liu H, Liu Z, Gao M, Hu X, Sun R, Shen X, et al. The effects of Daxx knockout on pluripotency and differentiation of mouse induced pluripotent stem cells. Cell Reprogram. 2020;22(2):90–8.
58. Devaiah BN, Gegonne A, Singer DS. Bromodomain 4: a cellular Swiss army knife. J Leukoc Biol. 2016;100(4):679–86.
59. You J, Li Q, Wu C, Kim J, Ottinger M, Howley PM. Regulation of aurora B expression by the bromodomain protein Brd4. Mol Cell Biol. 2009;29(18):5094–103.
60. Wu SY, Lee AY, Hou SY, Kemper JK, Erdjument-Bromage H, Tempst P, et al. Brd4 links chromatin targeting to HPV transcriptional silencing. Genes Dev. 2006;20(17):2383–96.
61. Roe JS, Mercan F, Rivera K, Pappin DJ, Vakoc CR. BET bromodomain inhibition suppresses the function of hematopoietic transcription factors in acute myeloid leukemia. Mol Cell. 2015;58(6):1028–39.
62. Filippakopoulos P, Knapp S. The bromodomain interaction module. FEBS Lett. 2012;586(17):2692–704.

63. Czerwinska P, Mazurek S, Wiznerowicz M. Application of induced pluripotency in cancer studies. Rep Pract Oncol Radiother. 2018;23(3):207–14.
64. Wang M, Lemos B. Ribosomal DNA copy number amplification and loss in human cancers is linked to tumor genetic context, nucleolus activity, and proliferation. PLoS Genet. 2017;13(9): e1006994.
65. Donati B, Lorenzini E, Ciarrocchi A. BRD4 and cancer: going beyond transcriptional regulation. Mol Cancer. 2018;17(1):164.

Publisher's Note